Article

Carbon Nanotube PtSn Nanoparticles for Enhanced Complete Biocatalytic Oxidation of Ethylene Glycol in Biofuel Cells

Jesimiel Glaycon Rodrigues Antonio, Jefferson Honorio Franco, Paula Z. Almeida, Thiago S. Almeida, Maria de Lourdes Teixeira de Morais Polizeli, Shelley D. Minteer, and Adalgisa Rodrigues de Andrade*

Read Online

ACCESS | Metrics & More | Article Recommendations | Supporting Information

ABSTRACT: We report a hybrid catalytic system containing metallic PtSn nanoparticles deposited on multiwalled carbon nanotubes ($Pt_{65}Sn_{35}$/MWCNTs), prepared by the microwave-assisted method, coupled to the enzyme oxalate oxidase (OxOx) for complete ethylene glycol (EG) electrooxidation. $Pt_{65}Sn_{35}$/MWCNTs, without OxOx, showed good electrochemical activity toward EG oxidation and all the byproducts. $Pt_{65}Sn_{35}$/MWCNTs cleaved the glyoxilic acid C−C bond, producing CO_2 and formic acid, which was further oxidized at the electrode. Concerning EG oxidation, the catalytic activity of the hybrid system ($Pt_{65}Sn_{35}$/MWCNTs+OxOx) was twice the catalytic activity of $Pt_{65}Sn_{35}$/MWCNTs. Long-term electrolysis revealed that $Pt_{65}Sn_{35}$/MWCNTs+OxOx was much more active for EG oxidation than $Pt_{65}Sn_{35}$/MWCNTs: the charge increased by 65%. The chromatographic results proved that $Pt_{65}Sn_{35}$/MWCNTs+OxOx collected all of the 10 electrons per molecule of the fuel and was able to catalyze EG oxidation to CO_2 due to the associative oxidation between the metallic nanoparticles and the enzymatic pathway. Overall, $Pt_{65}Sn_{35}$/MWCNTs+OxOx proved to be a promising system to enhance the development of enzymatic biofuel cells for further application in the bioelectrochemistry field.

KEYWORDS: Ethylene glycol, Oxalate oxidase, PtSn nanocatalyst, Enzymatic biofuel cell, hybrid catalyst
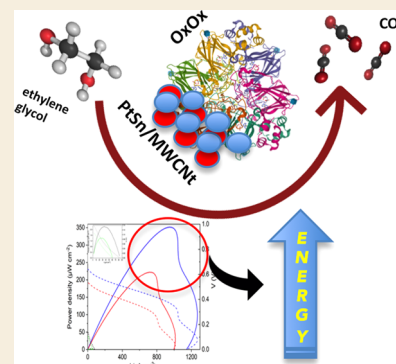
1. INTRODUCTION

Biofuel cells (BFCs) can generate electrical energy from electrochemical reactions involving microorganisms or enzymes as catalysts.[1] The main application of the BFC is to supply energy to devices that demand low power such as self-powered sensors and implantable or wearable devices, such as contact lenses, watches, and pacemakers. A good review of the perspective of these devices can be found in the literature.[2,3] Several types of fuels, such as glucose,[4,5] glycerol,[6−8] methanol,[9] ethanol,[10−13] ethylene glycol,[14] and lactate,[15] have been oxidized in BFCs to produce clean energy.[16] Nevertheless, the lower power density obtained in these devices has limited the application of enzymatic biofuel cells (EBFCs). To overcome this issue, the EBFC power density must be increased by harnessing the maximum number of electrons available in the fuel.[15] To achieve this goal, two approaches are generally used in an EBFC. First, an enzyme cascade is immobilized on the electrode surface, to promote complete glucose,[17] methanol,[9] lactate,[15] or ethanol[18] oxidation. Although this system generates a higher amount of energy, the large number of enzymes immobilized at the electrode surface decreases the chemical stability of the system.[11] The second approach, which has been studied more recently by our group, employs a hybrid system that combines the advantages of small organic catalysts (TEMPO, 2,2,6,6-tetramethylpiperidine 1-oxyl) or metallic nanocatalysts

with an enzyme or enzymes to withdraw higher energy from the biofuel and to generate higher power densities.[13] Metallic nanomaterials have been widely applied in electrocatalysts.[19,20] Metallic nanoparticles deposited on multiwalled nanotubes (MWCNTs) have been added to hybrid systems containing alcohol dehydrogenase (ADH) or glucose oxidase (GOx) for ethanol[12] and glucose[21] oxidation, respectively. The introduction of metallic nanoparticles to the bioanode structure improved fuel oxidation. Despite the higher energy output observed for these systems, they failed to harvest all of the available electrons from the fuel because the employed enzyme was designed to promote selective mild oxidation (2 electrons). For total oxidation to be obtained, the C−C bonds must be cleaved, which requires the use of enzymes like oxalate oxidase (OxOx)[7,10] or oxalate decarboxylase (OxDc).[8,22] These enzymes can cleave carbon−carbon bonds of simple carboxylic acids such as oxalic acid, glyoxylic acid, maleic acid, and mesoxalic acid, catalyzing oxalate oxidation to carbon dioxide (CO_2).[6,7,10,23,24] However, these enzymes

cannot oxidize alcohols directly or obtain total oxidation of these fuels. In this context, a hybrid architecture has been reported for ethanol[10,13,22] and glycerol[7,8] with satisfactory results.

Ethylene glycol (EG) is an interesting fuel source, because of its high energy density (5.3 kWh kg^{-1}).[25] This symmetric diol is considered a model system for the oxidation of diols and bifunctional molecules.[26] Another advantage is its higher boiling point (197 °C) as compared to methanol (64.7 °C) and ethanol (78.2 °C). Nonetheless, EG has rarely been used as a fuel in a BFC, and just one investigation employing EG has been reported. Falase et al.[14] immobilized ADH onto an electropolymerized film consisting of methylene green (PMG), multiwalled carbon nanotubes (MWCNTs), and nanostructured PtRu and reported that the current density for EG oxidation at the hybrid system (PMG-PtRu-ADH) was 1.2 times higher as compared to PMG-ADH.

Here, we report a hybrid system for complete EG oxidation. We immobilized PtSn nanoparticles on MWCNTs to oxidize the diol, and we employed the enzyme OxOx to break the C−C bonds of the product formed after the action of PtSn/MWCNTs. We conducted electrochemical and chromatographic experiments to demonstrate the capacity of the combined Pt$_{65}$Sn$_{35}$/MWCNTs and OxOx system to completely oxidize EG. Overall, we show that the power density of the fuel cell is enhanced through the use of a promising hybrid system that has never been employed for EG oxidation.

2. EXPERIMENTAL SECTION

2.1. Chemicals

Ethylene glycol (EG), glycolaldehyde, glycolic acid, glyoxylic acid, oxalic acid, bovine serum albumin (BSA), sulfuric acid, phosphoric acid, and citric acid were from Sigma-Aldrich. Carboxyl multiwalled carbon nanotubes (MWCNTs, OD ≤ 8 nm, ID = 2−5 nm, OL = 10−30 mm) were obtained from Cheap Tubes Inc. The enzyme OxOx was expressed and purified in our laboratory. The 150 mmol L^{-1} citric acid/phosphate buffer (pH = 5.5) and 50 mmol L^{-1} acetate buffer pH 4.0 were prepared by dissolving the appropriate amounts of salts in ultrapure water. The water used was from a Millipore Milli-Q system. All of the enzyme solutions were prepared and used immediately.

2.2. Enzymatic Assays

The enzyme OxOx was obtained as described previously[10,27] and stored at −80 °C in separate 500 μL Eppendorf tubes until use. The enzymatic activity of OxOx was determined as described before.[28] In a final volume of 1 mL, a solution containing 5 μM ABTS (2,2′-azino-bis(3-ethylbenzothiazoline-6-sulfonic acid) diammonium salt), 25 U HRP (peroxidase from horseradish), and 5 mM sodium oxalate was prepared in 50 mmol L^{-1} acetate buffer pH 4.0. During continuous reaction, absorbance was measured at 650 nm. The chromophore extinction coefficient was 10 000 L mol^{-1} cm^{-1}. The enzymatic solution presented an activity of 4.00 ± 0.07 U mL^{-1}. The amount of protein was determined with a Bradford assay.[29]

2.3. Metallic Nanoparticles Synthesis

Pt$_{75}$Sn$_{25}$/MWCNTs (Pt:Sn molar ratio) were prepared by the microwave-assisted method as described previously.[30,31] Briefly, 50 mg of the resulting material was obtained by adding 30 mL of propylene glycol (as a solvent and reduce agent), 1.14 mL of SnCl$_2$ (0.025 mol L^{-1}), 1.11 mL of H$_2$PtCl$_6$·6H$_2$O (0.077 mol L^{-1}), and 46.6 mg of sodium acetate to a 250 mL beaker under vigorous stirring for 5 min in an ultrasonic bath. Once the solution was dissolved and well mixed, 30 mg of MWCNTs, previously functionalized by refluxing 1.0 g of MWCNTs with 65% (w/w) HNO$_3$ at 90 °C for 5 h, was added to the solution to achieve a final catalytic material with 40% wt metal loading. This mixture was kept under ultrasound stirring (30 min) to obtain a homogeneous suspension. After the 30

min period, the mixture was transferred to a microwave oven (Panasonic NN-ST568WRU, 2450 Hz, 800 W), operating at 100% for 2 min. Finally, the carbon nanotubes were filtered through a 0.2 μm PTFE membrane and washed with ethanol (Merck) and acetone (Merck), respectively. At the end, the catalytic nanomaterial was dried for 2 h in an oven at 120 °C under inert atmosphere (0.5 L min^{-1} of nitrogen gas flow).

For comparison, Pt/MWCNTs were synthesized by the same experimental procedure described above, by adding 1.32 mL of 0.077 mol L^{-1} H$_2$PtCl$_6$·6H$_2$O (Aldrich) and 41.8 mg of sodium acetate to 30 mL of propylene glycol.

2.4. Catalyst Materials Analysis

Energy-dispersive X-ray spectroscopy (EDX) was performed on a Leica microscope Zeiss LEO 440 model scanning electron microscope coupled to an Oxford 7060 model analyzer. Diffraction patterns were acquired on a D5005 Siemens X-ray diffractometer that was operated with Cu Kα radiation (λ = 1.5406 Å) that was generated at 40 kV and 40 mA. The analyses were performed with the following static parameters: (1) 2θ range from 20° to 90°, (2) step of 0.03° s^{-1}, and (3) total analysis time of 1.97 h. Details of the measurement of the crystallite size (D), degree of the alloying (X$_M$) of the binary materials, and the XRD data treatment can be obtained as described before.[32]

2.5. Electrode Preparation

Two different noble metals were tested to prepare the hybrid bioanodes Pt/MWCNTs and Pt$_{65}$Sn$_{35}$/MWCNTs. The binary system Pt$_{65}$Sn$_{35}$/MWCNTs proved to be much more active for EG oxidation at lower overpotential, so the electrodes modified with Pt$_{65}$Sn$_{35}$/MWCNTs were used to prepare the hybrid systems herein. The catalytic ink was obtained by mixing 2 mg of Pt$_{65}$Sn$_{35}$/MWCNTs in 95 μL of isopropanol and 5 μL of 5% Nafion. Homogeneous ink was obtained by sonicating the mixture for 30 min. Then, either 20 μL of this emulsion was pipetted into a glass carbon with diameter of 7 mm and which had previously been mechanically polished for the cyclic voltammetry and power density curve experiment or 50 μL of this emulsion was pipetted into a carbon paper (Avcarb 75) electrode of 1 cm^2 for the electrolysis experiment. All the electrodes were dried in a desiccator for 12 h before being used.

2.6. Electrochemical Measurements

The voltammetric assays were conducted on an AUTOLAB potentiostat/galvanostat (software NOVA 1.11) employing a home-made Ag/AgCl reference electrode and a homemade Pt mesh counter electrode. Cyclic voltammetric (CV) experiments were measured while scanning at a rate of 10 mV s^{-1}. The I$_{peak}$ was calculated by the delta with the current generated in the electrolyte at that same potential. The supporting electrolyte was a pH 5.5 buffered solution of 150 mmol L^{-1} citric acid/phosphate buffer. In the assay involving the hybrid system of Pt$_{65}$Sn$_{35}$/MWCNTs+OxOx, 10 mL of electrochemical cell solution was spiked with 75 μL of the OxOx enzyme solution. The EG concentration was kept constant at 100 mmol L^{-1} unless otherwise stated. The chronoamperometric tests were carried out on the same electrochemical cell construction at a fixed potential (0.9 V vs Ag/AgCl); EG and oxidation products (oxalic acid, glyoxylic acid, and glycolic acid) were added at determined intervals to increase the concentration by 20 mmol L^{-1} until 200 mmol L^{-1} was reached.

2.7. Power Density Curves

Measurements of open-circuit voltage and power density were performed in a two-compartment cell, where the compartments were separated by a Nafion ion exchange membrane.[33] An air-breathing cathode was made by hot-pressing a Nafion 212 membrane to a gas diffusion electrode (A6ELAT/BASF) containing 20% by weight platinum on carbon. To establish the open-circuit voltage (OCV) of the cell, the electrodes were monitored for 20 min or until the OCV was stabilized. Then, a very slow (1 mV s^{-1}) linear sweep polarization was recorded from OCV to 0.0 V.

2.8. Electrolysis and Product Identification

For EG, bulk electrolysis experiments were conducted at a constant potential (0.500 V vs Ag/AgCl) for 12 and 72 h for the purely electrochemical ($Pt_{65}Sn_{35}$/MWCNTs) and the hybrid ($Pt_{65}Sn_{35}$/MWCNTs+OxOx) systems, respectively. A three-compartment electrolytic cell was used (Figure S1). The anodic compartment was filled with 12 mL of 150 mmol L^{-1} citric acid/phosphate buffer (pH = 5.5); this pH was chosen because it is in the optimum pH range for oxalate oxidase and similar values was already successfully applied in other hybrid systems with OxOx;[7,10] for the assays involving the hybrid system $Pt_{65}Sn_{35}$/MWCNTs+OxOx, 90 μL of OxOx solution was added. The EG concentration was kept constant (100 mmol L^{-1}) unless otherwise stated. Before the experiments, the anode compartment was purged with N_2 to completely remove carbon dioxide and oxygen from the solution. The Ag/AgCl reference electrode was placed in the anode compartment inside a Lugging-Haber capillary. The cathodic compartment only contained air to create an air-breathing cathode. To obtain further insight into the mechanism pathway followed by some of the identified EG oxidation products, that is, glycolic acid (GA), glyoxylic acid (GOA), formic acid (FA), oxalic acid (OA), and glycolaldehyde (GAld), assays were performed by employing $Pt_{65}Sn_{35}$/MWCNTs as the anode in the presence and absence of OxOx (0.03 U mL^{-1}); the potential was fixed at 0.500 V vs Ag/AgCl for 12 h. The same procedure was repeated with the hybrid system $Pt_{65}Sn_{35}$/MWCNTs+OxOx. Also, a purely enzymatic assay employing these products at 100 mmol L^{-1} was accomplished by adding 0.03 U mL^{-1} OxOx within a total reaction time of 24 h. The total volume of the solution containing previously deaerated supporting electrolyte was 5 mL. The system was kept closed.

A chromatograph system (Shimadzu, model LC-10AT) coupled to a double online UV detection system (λ = 210 nm) equipped with refractive index RID-10A detectors (RID-10A) and an autoinjector was used to analyze the products from the electrolysis. The following parameters were used: (i) isocratic elution through a Aminex HPX-87H (Bio-Rad) column; (ii) mobile phase of sulfuric acid (3.33 mmol L^{-1}); (iii) 0.6 mL min^{-1} flow rate, (iv) 20 μL injection volume, and (v) column temperature at 45 °C. To measure the generated CO_2, the collected sample was mixed with 0.1 mol L^{-1} NaOH at a 1:1 ratio, to form the Na_2CO_3 that can be measured in the refractive index detector. Standard anhydrous sodium carbonate solution (Aldrich) was used to identify CO_2 formed during the electrolysis. All of the other individual components were identified with commercial standards (HPLC grade).

3. RESULTS AND DISCUSSION

3.1. Nanomaterials Characterization of the Catalytic Material

EDX analysis reveals that the bulk composition of Pt:Sn molar ratio was $Pt_{65}Sn_{35}$. X-ray diffraction patterns of $Pt_{65}Sn_{35}$/MWCNTs and Pt/MWCNTs are shown in Figure 1. The peaks that are shown were characteristic of the crystalline structure of face-centered cubic (fcc) platinum (space group $Fm\bar{3}m$). This refers, respectively, to the reflection planes (111), (200), (220), (311), and (222) (red dashed lines) (JCPDS # 00-004-0802). The crystallite average size of the synthesized nanoparticles was 3.4 nm, obtained from XRD data plane (220). The peak at $2\theta = 25°$ is characteristic of the carbon from the support with the reflection plane at (002).

Compared to pure Pt/MWCNTs (black line), the 2θ diffraction peaks of $Pt_{65}Sn_{35}$/MWCNTs (blue line) indicated that Sn atoms were incorporated into the Pt structure, leading to a significant shift in the unit cell lattice parameter (a = 3.96800 Å) as compared to pure Pt (a = 3.91455 Å). We obtained a more reliable indication of Sn incorporation into Pt structure by calculating the degree of alloying by using Vegard's law. For $Pt_{65}Sn_{35}$/MWCNTs, the degree of Sn
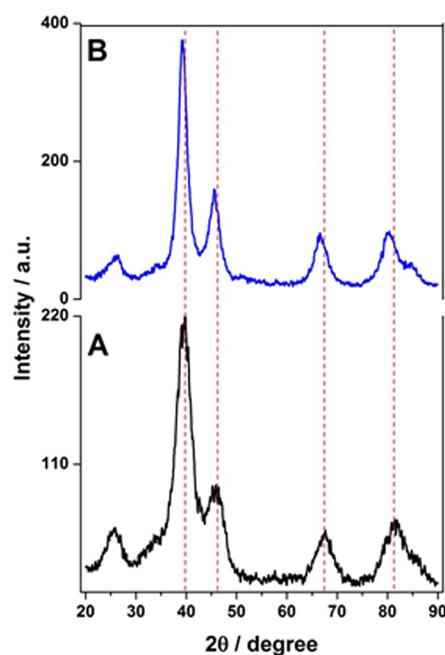

Figure 1. XRD data of the (A) Pt/MWCNT and (B) $Pt_{65}Sn_{35}$/MWCNTs nanoparticles prepared by the microwave method.

alloyed was 7.9%. As described in literature, this change in the catalyst structure can improve its electrochemical activity toward the oxidation of small molecules.[34−36]

3.2. Cyclic Voltammetry Experiments

First, we analyzed how the metallic catalyst affected EG oxidation. Figure S2 shows the cyclic voltammetry (CV) curve of the metallic catalysts ($Pt_{65}Sn_{35}$/MWCNT) and (Pt/MWCNTs) in the presence and absence of EG. In the absence of EG, we ascertained a small hydrogen adsorption/desorption peak for both catalysts; the H_2 peaks decreased at neutral pHs as compared to acidic medium.[31] We did not identify a large contribution of Sn nanoparticles in the CV of the supporting electrolyte (Figure S2). Nevertheless, in the presence of EG, a well-defined anodic peak emerged in the region of 0.4 V vs Ag/AgCl for $Pt_{65}Sn_{35}$/MWCNTs. The introduction of Sn shifted the onset oxidation potential of EG 50 mV toward less positive values (Figure S2). Sn is well-known for its good performance as a cocatalyst of Pt nanoparticles during alcohol oxidation.[37] Sn changes the electronic structure of Pt/MWCNTs, consequently altering the adsorption strength of the EG products formed on the Pt-sites and promoting their oxidation at less positive potentials.[37] Although both Pt/MWCNTs and $Pt_{65}Sn_{35}$/MWCNTs provided the same magnitude of current as revealed during the chronoamperometric titration tests performed at 0.5 vs Ag/AgCl (Figure S3), the potential shifted toward less negative values and the current decreased in the presence of $Pt_{65}Sn_{35}$-MWCNTs, indicating that it was less poisoned than Pt/MWCNTs. At intermediate EG concentrations, the current decreased more abruptly for Pt/MWCNTs than for $Pt_{65}Sn_{35}$/MWCNTs. This result indicated that the active sites became more strongly blocked in the absence of Sn as the oxidation proceeded.

To evaluate the role of the hybrid system $Pt_{65}Sn_{35}$/MWCNTs+OxOx in EG oxidation, we analyzed the CV curves in the presence and absence of the enzyme OxOx (Figure 2). In the absence of EG, the introduction of OxOx
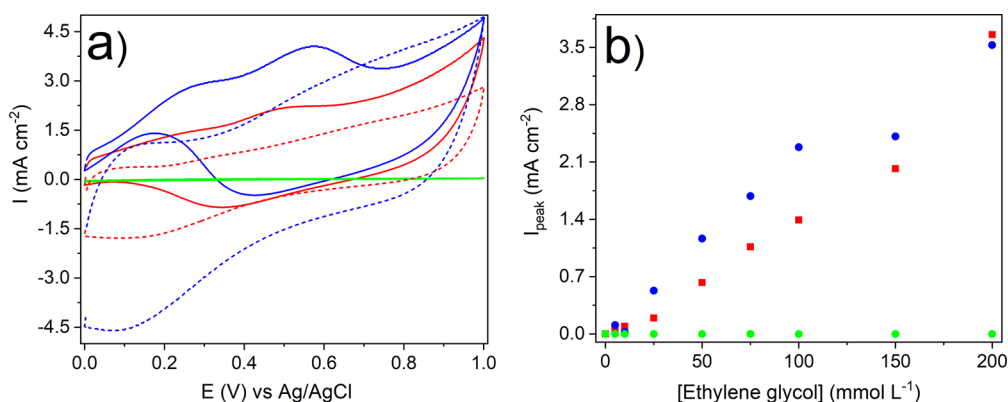
Figure 2. Cyclic voltammetry curves (A) and current peak (B) of EG in the presence of $Pt_{65}Sn_{35}$/MWCNTs+OxOx (blue/circle), $Pt_{65}Sn_{35}$/MWCNTs (red/square), or pure enzyme (carbon vitreous electrode in the presence of 0.03 U mL^{-1} OxOx) (green/circle). The solid lines refer to the presence of EG; the dashed lines refer to the absence of EG; supporting electrolyte of 150 mmol L^{-1} citric acid/phosphate buffer (pH = 5.5), [EG] = 100 mmol L^{-1}, [OxOx] = 0.03 U mL^{-1}, scan rate = 10 mV s^{-1}.
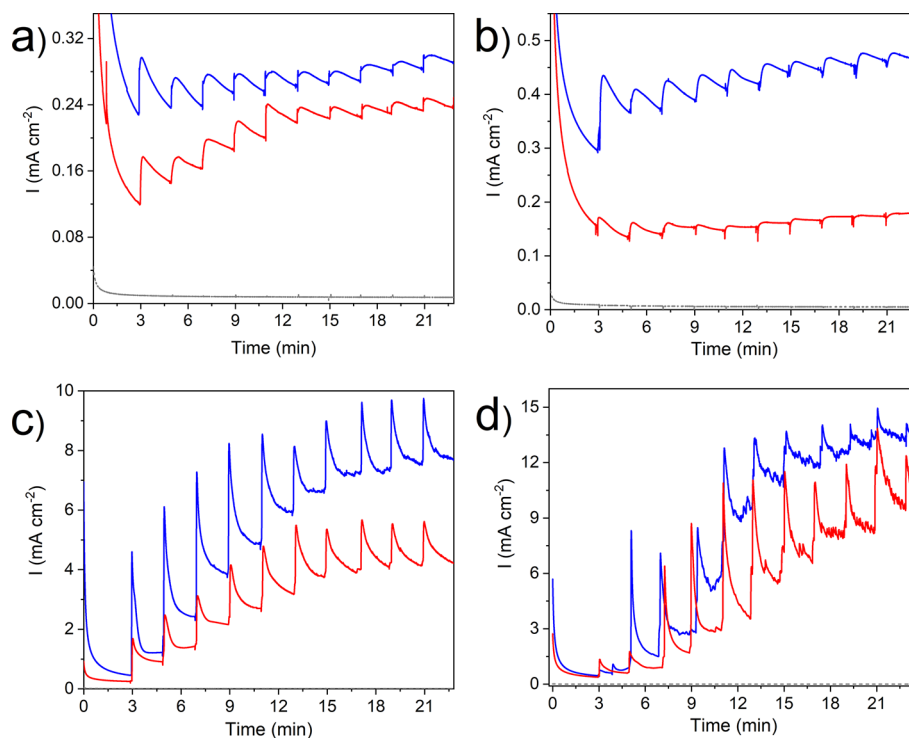

Figure 3. Chronoamperometric assay performed in the presence of $Pt_{65}Sn_{35}$/MWCNTs+OxOx (blue line), $Pt_{65}Sn_{35}$/MWCNTs (red line), and control experiment (carbon vitreous electrode in the electrolyte) (gray dash line). Successive additions of 20 mmol L^{-1} ethylene glycol (a), glycolic acid (b), glyoxylic acid (c), and oxalic acid (d) at a fixed oxidation potential (0.900 V vs Ag/AgCl). Supporting electrolyte of 150 mM citric acid/phosphate buffer (pH = 5.5), [OxOx] = 0.03 U mL^{-1}.

enhanced the capacitive current, indicating that the double layer changed with the introduction of the biomaterial into the solution. The EG peak current was placed at 40 mV more positive potentials in the presence of OxOx as compared to $Pt_{65}Sn_{35}$/MWCNTs. There was a straight correlation between the current peak and the EG concentration for both systems until 100 mmol L^{-1}. On average, the current densities observed in the presence of OxOx were 1.6 greater than the current densities observed for $Pt_{65}Sn_{35}$/MWCNTs. At higher concentrations, the current density remained similar for both systems. The catalytic activity generated by the hybrid system $Pt_{65}Sn_{35}$/MWCNTs+OxOx resembled the results reported by Falase et al.,[14] who reported a similar increase in the current density of

EG oxidation in the presence of PtRu-ADH, indicating the beneficial effect of the hybrid system.

Figure 2B shows the assay in the presence OxOx only (OxOx in solution and carbon vitreous anode, green/circle). The enzyme did not oxidize EG, confirming previous literature data[7,10] and proving that C−C bond cleavage in the enzymatic catabolic route requires previous oxidation of the alcohol. The respective CV is shown in the Supporting Information (Figure S4).

To understand how the enzyme OxOx mediates the oxidation steps in this hybrid system, we recorded chronoamperometric curves for $Pt_{65}Sn_{35}$/MWCNTs+OxOx and $Pt_{65}Sn_{35}$/MWCNTs upon successive injections of EG and its oxidation products (oxalic acid, glycolic acid, and glyoxylic

acid) at a controlled potential (0.9 V vs Ag/AgCl) (Figure 3). When the assays were conducted in the presence of $Pt_{65}Sn_{35}$/MWCNTs+OxOx, the current increased for all the analyzed compounds as compared to $Pt_{65}Sn_{35}$/MWCNTs. In the case of EG, the increased current in the presence of $Pt_{65}Sn_{35}$/MWCNTs+OxOx (Figure 3a) could be explained by analyzing the profile of the oxidation products at $Pt_{65}Sn_{35}$/MWCNTs (Figure 3b−d). The OxOx activity regarding glycolic, glyoxylic, and oxalic acids has already been described as resulting from the ability of OxOx to react with these compounds.[7,23,24] Thus, the increased current for EG in the presence of $Pt_{65}Sn_{35}$/MWCNTs+OxOx could be rationalized in terms of a chain reaction with the products generated by $Pt_{65}Sn_{35}$/MWCNTs, e.g., glycolic, glyoxylic, and oxalic acids, which further reacted with OxOx. In contrast to what occurs in the case of ethanol,[10] when both the organic catalyst (TEMPO-LPEI) and the enzyme were immobilized on the electrode surface, in the assays conducted herein, OxOx was in solution, so the generated product must have diffused away from the electrode interface to reach the enzyme. This could account for the lower response in terms of the current increase observed in the CVs.

3.3. Electrolysis and Product Analysis

To quantify and to identify the reaction products, we carried out long-term EG electrolysis at 0.5 V vs Ag/AgCl for 72 h for the different systems. We analyzed the products from bulk EG electrolysis in the presence of $Pt_{65}Sn_{35}$/MWCNTs, $Pt_{65}Sn_{35}$/MWCNTs+OxOx, or MWCNTs/C+OxOx by HPLC-UV/RID. Figure 4 displays the chronoamperometric curves.
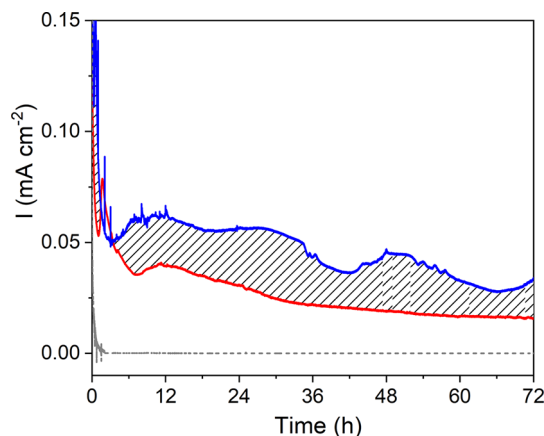

Figure 4. Amperometric $i−t$ curves that were measured during long-term bulk EG electrolysis in the presence of $Pt_{65}Sn_{35}$/MWCNTs+OxOx (blue line), $Pt_{65}Sn_{35}$/MWCNTs (red line), and pure enzyme (carbon paper electrode in the presence of 0.03 U mL^{-1} OxOx) (green line) and control experiment ($Pt_{65}Sn_{35}$/MWCNTs+OxOx in the electrolyte) (gray dashed line). Supporting electrolyte of 150 mmol L^{-1} citric acid/phosphate buffer (pH = 5.5), [EG] = 100 mmol L^{-1}, Eap = 0.5 V vs Ag/AgCl, [OxOx] = 0.03 U mL^{-1}.

As expected, the current density for EG oxidation at $Pt_{65}Sn_{35}$/MWCNTs+OxOx was higher as compared to the current density for EG oxidation at $Pt_{65}Sn_{35}$/MWCNTs. As for the enzymatic assay, there was no evidence of EG oxidation. Figure 4 also highlights the total charge gain obtained with $Pt_{65}Sn_{35}$/MWCNTs+OxOx, which corresponded to 5.5 coulombs. This represented a 65% increase in the total charge as compared to $Pt_{65}Sn_{35}$/MWCNTs. Thus, $Pt_{65}Sn_{35}$/MWCNTs+OxOx was much more active toward EG oxidation

than $Pt_{65}Sn_{35}$/MWCNTs, indicating that OxOx can oxidize the products formed by $Pt_{65}Sn_{35}$/MWCNTs by harvesting more electrons from the system. To verify whether citric acid from the buffer could be oxidized during the electrolysis, we performed a control experiment in the absence of the fuel. No product or current was generated under this condition as previously reported by our group.[10]

Figure 5 displays the distribution of the products from long-term (12 h) EG electrolysis. We detected two from EG
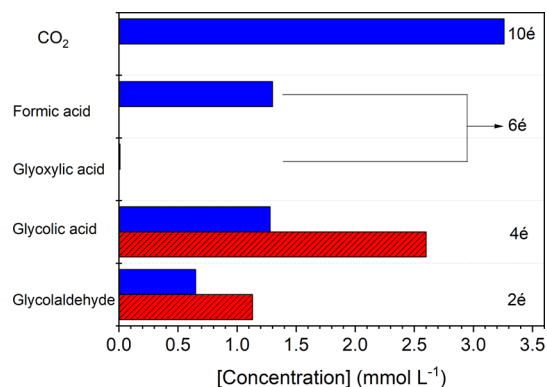

Figure 5. Distribution of products from EG oxidation (100 mmol L^{-1}) after electrolysis for 12 h at $Pt_{65}Sn_{35}$/MWCNTs+OxOx (blue) and $Pt_{65}Sn_{35}$/MWCNTs (red). Support electrolyte of 150 mmol L^{-1} citric acid/phosphate buffer (pH = 5.5), [OxOx] = 0.03 U mL^{-1}, Eap = 0.5 V versus Ag/AgCl.

electrooxidation at $Pt_{65}Sn_{35}$/MWCNTs: GA (2.6 mmol L^{-1}) and GAld (1.13 mmol L^{-1}). There was no evidence of carbon−carbon bonds or other more oxidizable acids. On the other hand, electrolysis in the presence of $Pt_{65}Sn_{35}$/MWCNTs+OxOx furnished five products. Among them, a considerable amount of C1 products emerged: CO_2 (3.26 mmol L^{-1}) and FA (1.3 mmol L^{-1}), demonstrating that OxOx can break the C−C bond of the oxidation products generated by electrochemical oxidation at $Pt_{65}Sn_{35}$/MWCNTs. Besides that, a smaller amount of GAld (0.65 mmol L^{-1}) and GA (1.28 mmol L^{-1}) and traces of GOA (10 μmol L^{-1}) were obtained. To explain this, it must be considered that the PtSn-catalyst and the enzyme acted in line, completely oxidizing the EG molecule and opening the possibility for all the 10 electrons available in this fuel to be harvested. We did not detect OA because its HPLC peak was hidden by the peak of the supporting electrolyte (sodium citrate).

To enhance the quantity of reaction products originating from EG electrooxidation, we extended the electrolysis time to 72 h. Longer reaction time did not affect product distribution, but it allowed traces of GOA in the PtSn catalyst to be recovered. The small amount of this product led us to infer that GOA underwent very fast oxidation as soon as it emerged, so it did not accumulate in the solution. Moreover, formic acid was consumed, indicating that longer electrolysis time allowed this compound to diffuse toward $Pt_{65}Sn_{35}$/MWCNTs electrode and to be reoxidized to CO_2, as described previously.[38,39]

Our group has already reported evidence of complete fuel oxidation in the presence of MWCNTs-COOH/TEMPO-LPEI/OxOx for ethanol[10] and TEMPO-NH$_2$+OxOx for glycerol.[7] Most of the time, investigations of EG oxidation at Pt-based catalyst have been conducted under drastic conditions such as extremely acidic or basic medium.[40] Studies
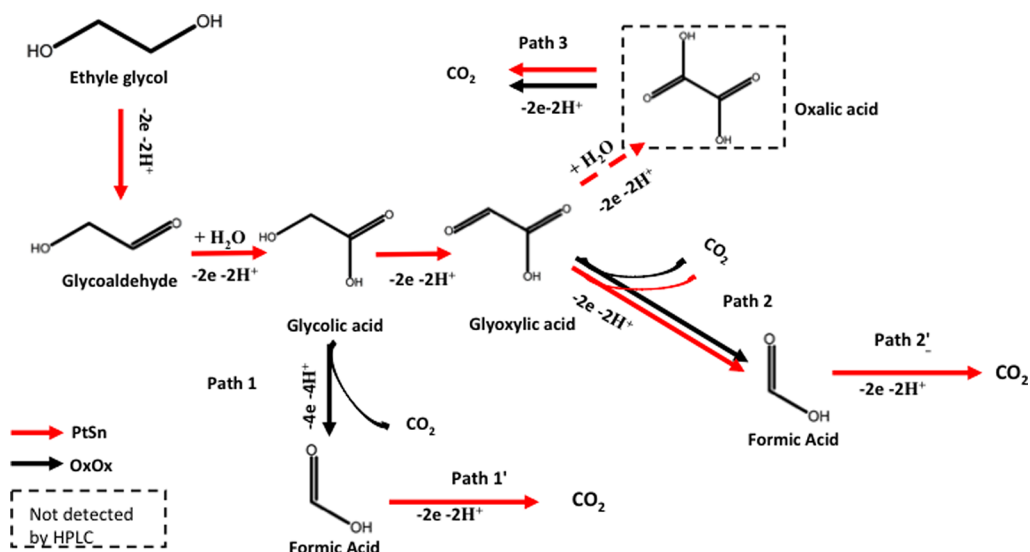
Figure 6. Proposed cascade mechanism for ethylene glycol oxidation at the hybrid electrode system $Pt_{65}Sn_{35}$/MWCNTs+OxOx. Oxidation mediated by $Pt_{65}Sn_{35}$ (red line) and bioenzymatic oxidation mediated by OxOx (black line).

based on spectral electrochemical techniques have provided evidence of carbon−carbon bond cleavage.[41] However, the main products were carbon acids (oxalic, glyoxylic, and glycolic acids), resulting from partial oxidation of the C2 products at the Pt-based catalysts.[40,41] The use of Pt-based catalysts coupled with the enzymatic pathway extends the possibility of applying this technology to a large number of systems.[42]

Because bioelectrochemical systems generate small currents, comparing the results obtained with electrochemical techniques and analytical experiments is difficult. Some authors have been successful at doing so for ethanol,[10,13,22] lactate,[43] and glycerol[7,8] oxidation. However, this is the first time that this kind of study has been reported for EG.

To elucidate the catalytic route of EG oxidation at $Pt_{65}Sn_{35}$/MWCNTs+OxOx and to understand the role of the catalyst, we examined the oxidation of the EG electrooxidation products via a purely enzymatic pathway (0.03 U mL^{-1}), at $Pt_{65}Sn_{35}$/MWCNTs, and at $Pt_{65}Sn_{35}$/MWCNTs+OxOx in the same conditions described for EG. Figure 6 illustrates the reaction pathway proposed for EG oxidation, and the results are depicted in Table S1. In the purely enzymatic assay with OA, the only product was CO_2 given that oxalate oxidase is highly specific for oxalate.[23,24] The enzyme also reacted with GA and GOA, cleaving these C2 acids, respectively, to CO_2 and FA; OxOx does not react with FA or the aldehyde (GAld). OxOx has been demonstrated to react with other acids other than its substrate, e.g., GOA,[7] maleic acid,[23] and mesoxalic acid.[6]

In the pure electrolytic pathway, i.e., in the presence of $Pt_{65}Sn_{35}$/MWCNTs, GAld electrooxidation gave 34.2% GA and traces of GOA, GA electrooxidation produced 68.0% GOA, GOA was electrooxidized to CO_2 (71.5%) and FA (12.4%), FA electrooxidation gave 22.0% CO_2, and finally OA gave 10.8% CO_2.

Following the oxidation of each product (Supporting Information), one can infer that $Pt_{65}Sn_{35}$/MWCNTs oxidized EG to 2-C products (GAld and the C2-acids) under mild pH (5.5) and oxidation potential (0.5 V vs Ag/AgCl). Once GOA was formed, it was rapidly electrooxidized to FA and CO_2 through routes 1' and 2'. The good CO_2 yield in the presence of $Pt_{65}Sn_{35}$/MWCNTs+OxOx was due to the concomitant

reaction of OxOx with GOA and GA, which cleaved the C−C bonds and gave FA (6 electrons) and CO_2 (10 electrons). Further oxidation of the remaining FA to CO_2 occurred by an electrochemical route at $Pt_{65}Sn_{35}$/MWCNTs. The reactivity of GOA with both catalysts explained the low yield of this product (Figure 5); GOA did not remain in the solution, but it was rapidly transformed into C1 products.

3.4. Power Density Test

We performed power curve experiments in the presence and absence of EG for $Pt_{65}Sn_{35}$/MWCNTs and $Pt_{65}Sn_{35}$/MWCNTs+OxOx (Figure 7). $Pt_{65}Sn_{35}$/MWCNTs+OxOx
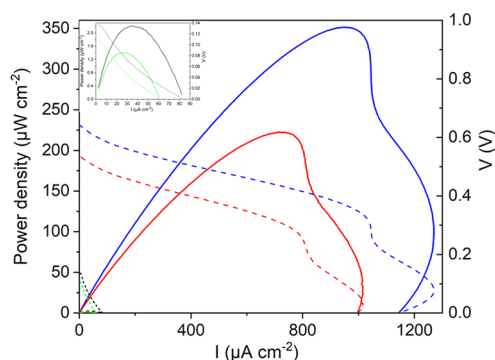

Figure 7. Power density curves of ethylene glycol/O_2 biofuel cell employing the hybrid system ($Pt_{65}Sn_{35}$/MWCNTs+OxOx) (blue line) and the metallic system ($Pt_{65}Sn_{35}$/MWCNTs) (red line) (100 mmol L^{-1} EG). Inset: profile in the absence of EG (green, $Pt_{65}Sn_{35}$/MWCNTs; black, $Pt_{65}Sn_{35}$/MWCNTs+OxOx). Supporting electrolyte of 150 mmol L^{-1} citric acid/phosphate buffer (pH = 5.5), scan rate of 1 mV s^{-1}, [OxOx] = 0.03 U mL^{-1}.

furnished a maximum current density of 930 ± 85 μA cm^{-2}, power density of 332 ± 28 μW cm^{-2}, and OCV of 0.643 ± 0.020 V. In the polarization curves, the current values obtained for $Pt_{65}Sn_{35}$/MWCNTs+OxOx were significantly compared to $Pt_{65}Sn_{35}$/MWCNTs: the current density increase was 28%, power increments were 38%, and the OCV was 18% higher. These results confirmed the significantly enhanced perform-

ance of $Pt_{65}Sn_{35}$/MWCNTs+OxOx in harvesting electrons from EG.

Table 1 summarizes some power density data for hybrid systems with small alcohols. To analyze these data, one must

Table 1. OCV (V) and Maximum Power Density for Hybrid Systems

hybrid system	fuel (mmol L^{-1})	OCP (V)	PD (μW cm^{-2})	ref
$Pt_{65}Sn_{35}$/MWCNTs+OxOx	EG	0.643	332	this work
amino-TEMPO/OxDc	EtOH	0.468	78.0	44
MWCNT-COOH/TEMPO-LPEI/OxOx	EtOH	0.492	302.5	10
ADH/TiO$_2$NTs-TCPP	EtOH	1.13	270	45
MWCNTs-COOH-Au/ADH	EtOH	0.61	155	12
MWCNT-NH$_2$-Au nanoparticles/ADH	EtOH	a	226	46
poly(MG-PYR) + MWCNTs + Nafion + ADH/AldDH/NAD$^+$	EtOH	0.503	275	47
MG+Nafion+ADH/AldDH/NAD$^+$	EtOH	0.510	390	48

^{a}Value not informed.

be aware that differences in experimental parameters may introduce severe distortions in the analysis. The values we obtained for $Pt_{65}Sn_{35}$/MWCNTs+OxOx, however, were in the same order of magnitude as the highest reported values. Herein, the power density generated by a hybrid system employing an inorganic catalyst ($Pt_{65}Sn_{35}$/MWCNTs+OxOx) instead of an organic catalyst, like TEMPO, proved innovative and promising. The energy gain obtained with $Pt_{65}Sn_{35}$/MWCNTs+OxOx revealed the excellent behavior of $Pt_{65}Sn_{35}$/MWCNTs associated with the enzymatic pathway, providing improved current density and power density. Notably, $Pt_{65}Sn_{35}$/MWCNTs could replace the organic catalyst (MWCNTs/TEMPO-LPEI MWCNTs/amino-TEMPO) in the hybrid system because of its superior energy efficiency and easy preparation.

Therefore, the hybrid system $Pt_{65}Sn_{35}$/MWCNTs+OxOx developed herein opens opportunities for improving the development of biofuel cells from different types of catalysts and fuels. This new approach can be applied to enhance energy generation and its management, allowing small devices with an extended lifetime to be implemented.

4. CONCLUSION

For the first time, we have demonstrated that $Pt_{65}Sn_{35}$/MWCNTs+OxOx can be applied to oxidize ethylene glycol completely. We have elucidated the electrocatalytic cascade for ethylene glycol oxidation at $Pt_{65}Sn_{35}$/MWCNTs+OxOx by investigating the electrochemical and the enzymatic routes for all the generated products. $Pt_{65}Sn_{35}$/MWCNTs can electro-oxidize EG to GAld (2 electrons) and 2C acids. Among these acids, $Pt_{65}Sn_{35}$/MWCNTs can cleave the C−C bonds of GOA to furnish FA and CO_2. OxOx not only reacts with its substrate (OA), but it also cleaves the C−C bond of GA and GOA, enhancing the CO_2 yield. In summary, the biocatalytic system harvests all 10 electrons from EG and improves the oxidation of the C2 products generated at $Pt_{65}Sn_{35}$/MWCNTs. The OCV (0.643 V) and power density (332 μW cm^{-2}) obtained herein are as high as the values obtained for some hybrid

systems reported in the literature with the advantage that our system is more stable and easier to prepare. In conclusion, we have described the potential of hybrid biofuel cells for application in electronic devices.

■ ASSOCIATED CONTENT

⑤ⓘ Supporting Information

The Supporting Information is available free of charge at https://pubs.acs.org/doi/10.1021/acsmaterialsau.1c00029.

Additional experimental details, including photographs of experimental setup, cyclic voltammetric curves and chronoamperometric assay of Pt/MWCNTs and $Pt_{65}Sn_{35}$/MWCNTs, electrochemical and enzymatic assay for subproducts of EG oxidation (PDF)

■ AUTHOR INFORMATION

Corresponding Author

Adalgisa Rodrigues de Andrade − *Department of Chemistry, Faculty of Philosophy Sciences and Letters at Ribeirão Preto, University of São Paulo, 14040-901 Ribeirão Preto, SP, Brazil;* ⓘ orcid.org/0000-0002-4121-0384; Phone: +55-16-3315-3725; Email: ardandra@ffclrp.usp.br

Authors

Jesimiel Glaycon Rodrigues Antonio − *Department of Chemistry, Faculty of Philosophy Sciences and Letters at Ribeirão Preto, University of São Paulo, 14040-901 Ribeirão Preto, SP, Brazil;* ⓘ orcid.org/0000-0002-7437-8298

Jefferson Honorio Franco − *Department of Chemistry, Faculty of Philosophy Sciences and Letters at Ribeirão Preto, University of São Paulo, 14040-901 Ribeirão Preto, SP, Brazil*

Paula Z. Almeida − *Department of Biology, Faculty of Philosophy Sciences and Letters at Ribeirão Preto, University of São Paulo, 14040-901 Ribeirão Preto, SP, Brazil*

Thiago S. Almeida − *Department of Chemistry, Faculty of Philosophy Sciences and Letters at Ribeirão Preto, University of São Paulo, 14040-901 Ribeirão Preto, SP, Brazil; Department of Chemistry, Campus Universitário de Iturama, Universidade Federal do Triângulo Mineiro, 38280-000 Iturama, MG, Brazil*

Maria de Lourdes Teixeira de Morais Polizeli − *Department of Biology, Faculty of Philosophy Sciences and Letters at Ribeirão Preto, University of São Paulo, 14040-901 Ribeirão Preto, SP, Brazil*

Shelley D. Minteer − *Department of Chemistry, University of Utah, Salt Lake City, Utah 84112, United States;* ⓘ orcid.org/0000-0002-5788-2249

Complete contact information is available at:
https://pubs.acs.org/10.1021/acsmaterialsau.1c00029

Notes

The authors declare no competing financial interest.

■ REFERENCES

(1) Rasmussen, M.; Abdellaoui, S.; Minteer, S. D. Enzymatic biofuel cells: 30 years of critical advancements. *Biosens. Bioelectron.* **2016**, *76*, 91−102.

(2) Katz, E.; Bollella, P. Fuel Cells and Biofuel Cells: From Past to Perspectives. *Isr. J. Chem.* **2021**, *61*, 68−84.

(3) Jeerapan, I.; Sempionatto, J. R.; Wang, J. On-Body Bioelectronics: Wearable Biofuel Cells for Bioenergy Harvesting and Self-Powered Biosensing. *Adv. Funct. Mater.* **2020**, *30*, 1906243.

(4) Xu, S.; Minteer, S. D. Enzymatic Biofuel Cell for Oxidation of Glucose to CO 2. *ACS Catal.* **2012**, *2*, 91−94.

(5) Kang, Z.; Job Zhang, Y.-H. P.; Zhu, Z. A shriveled rectangular carbon tube with the concave surface for high-performance enzymatic glucose/O2 biofuel cells. *Biosens. Bioelectron.* **2019**, *132*, 76−83.

(6) Arechederra, R. L.; Minteer, S. D. Complete Oxidation of Glycerol in an Enzymatic Biofuel Cell. *Fuel Cells* **2009**, *9*, 63−69.

(7) Hickey, D. P.; McCammant, M. S.; Giroud, F.; Sigman, M. S.; Minteer, S. D. Hybrid Enzymatic and Organic Electrocatalytic Cascade for the Complete Oxidation of Glycerol. *J. Am. Chem. Soc.* **2014**, *136*, 15917−15920.

(8) Macazo, F. C.; Hickey, D. P.; Abdellaoui, S.; Sigman, M. S.; Minteer, S. D. Polymer-immobilized, hybrid multi-catalyst architecture for enhanced electrochemical oxidation of glycerol. *Chem. Commun.* **2017**, *53*, 10310−10313.

(9) Wu, G.; Gao, Y.; Zhao, D.; Ling, P.; Gao, F. Methanol/Oxygen Enzymatic Biofuel Cell Using Laccase and NAD + -Dependent Dehydrogenase Cascades as Biocatalysts on Carbon Nanodots Electrodes. *ACS Appl. Mater. Interfaces* **2017**, *9*, 40978−40986.

(10) Franco, J. H.; de Almeida, P. Z.; Abdellaoui, S.; Hickey, D. P.; Ciancaglini, P.; de Lourdes T. M. Polizeli, M.; Minteer, S. D.; de Andrade, A. R. Bioinspired architecture of a hybrid bifunctional enzymatic/organic electrocatalyst for complete ethanol oxidation. *Bioelectrochemistry* **2019**, *130*, 107331.

(11) Aquino Neto, S.; Minteer, S. D.; de Andrade, A. R. Developing ethanol bioanodes using a hydrophobically modified linear polyethylenimine hydrogel for immobilizing an enzyme cascade. *J. Electroanal. Chem.* **2018**, *812*, 153−158.

(12) Aquino Neto, S.; Almeida, T. S.; Palma, L. M.; Minteer, S. D.; de Andrade, A. R. Hybrid nanocatalysts containing enzymes and metallic nanoparticles for ethanol/O2 biofuel cell. *J. Power Sources* **2014**, *259*, 25−32.

(13) Franco, J. H.; Neto, S. A.; Hickey, D. P.; Minteer, S. D.; de Andrade, A. R. Hybrid catalyst cascade architecture enhancement for complete ethanol electrochemical oxidation. *Biosens. Bioelectron.* **2018**, *121*, 281−286.

(14) Falase, A.; Garcia, K.; Lau, C.; Roy, J.; Atanassov, P. Hybrid Nano-Structured Platinum-Based Catalyst/Enzyme Anode for Oxidation of Ethanol and Ethylene Glycol. *ECS Electrochem. Lett.* **2012**, *1*, F9−F11.

(15) Sokic-Lazic, D.; de Andrade, A. R.; Minteer, S. D. Utilization of enzyme cascades for complete oxidation of lactate in an enzymatic biofuel cell. *Electrochim. Acta* **2011**, *56*, 10772−10775.

(16) Xiao, X.; Xia, H.; Wu, R.; Bai, L.; Yan, L.; Magner, E.; Cosnier, S.; Lojou, E.; Zhu, Z.; Liu, A. Tackling the Challenges of Enzymatic (Bio)Fuel Cells. *Chem. Rev.* **2019**, *119*, 9509−9558.

(17) Xu, S.; Minteer, S. D. Enzymatic Biofuel Cell for Oxidation of Glucose to CO2. *ACS Catal.* **2012**, *2*, 91−94.

(18) Sokic-Lazic, D.; Minteer, S. D. Citric acid cycle biomimic on a carbon electrode. *Biosens. Bioelectron.* **2008**, *24*, 939−944.

(19) Xu, H.; Shang, H.; Wang, C.; Du, Y. Ultrafine Pt-Based Nanowires for Advanced Catalysis. *Adv. Funct. Mater.* **2020**, *30*, 2000793.

(20) Xu, H.; Shang, H.; Wang, C.; Du, Y. Low-Dimensional Metallic Nanomaterials for Advanced Electrocatalysis. *Adv. Funct. Mater.* **2020**, *30*, 2006317.

(21) Aquino Neto, S.; Milton, R. D.; Crepaldi, L. B.; Hickey, D. P.; de Andrade, A. R.; Minteer, S. D. Co-immobilization of gold nanoparticles with glucose oxidase to improve bioelectrocatalytic glucose oxidation. *J. Power Sources* **2015**, *285*, 493−498.

(22) Franco, J. H.; Klunder, K. J.; Lee, J.; Russell, V.; de Andrade, A. R.; Minteer, S. D. Enhanced electrochemical oxidation of ethanol using a hybrid catalyst cascade architecture containing pyrene-TEMPO, oxalate decarboxylase and carboxylated multi-walled carbon nanotube. *Biosens. Bioelectron.* **2020**, *154*, 112077.

(23) KOYAMA, H. Purification and characterization of oxalate oxidase from Pseudomonas sp. OX-53. *Agric. Biol. Chem.* **1988**, *52*, 743−748.

(24) Rana, H.; Moussatche, P.; Rocha, L. S.; Abdellaoui, S.; Minteer, S. D.; Moomaw, E. W. Isothermal titration calorimetry uncovers substrate promiscuity of bicupin oxalate oxidase from Ceriporiopsis subvermispora. *Biochem. Biophys. Reports.* **2016**, *5*, 396−400.

(25) Ozoemena, K. I. Nanostructured platinum-free electrocatalysts in alkaline direct alcohol fuel cells: catalyst design, principles and applications. *RSC Adv.* **2016**, *6*, 89523−89550.

(26) Schnaidt, J.; Heinen, M.; Jusys, Z.; Behm, R. J. Oxidation of the Partly Oxidized Ethylene Glycol Oxidation Products Glycolaldehyde, Glyoxal, Glycolic Acid, Glyoxylic Acid, and Oxalic Acid on Pt Electrodes: A Combined ATR-FTIRS and DEMS Spectroelectrochemical Study. *J. Phys. Chem. C* **2013**, *117*, 12689−12701.

(27) Moussatche, P.; Angerhofer, A.; Imaram, W.; Hoffer, E.; Uberto, K.; Brooks, C.; Bruce, C.; Sledge, D.; Richards, N. G. J.; Moomaw, E. W. Characterization of Ceriporiopsis subvermispora bicupin oxalate oxidase expressed in Pichia pastoris. *Arch. Biochem. Biophys.* **2011**, *509*, 100−107.

(28) REQUENA, L.; BORNEMANN, S. Barley (Hordeum vulgare) oxalate oxidase is a manganese-containing enzyme. *Biochem. J.* **1999**, *343*, 185−190.

(29) Bradford, M. M. A rapid and sensitive method for the quantitation of microgram quantities of protein utilizing the principle of protein-dye binding. *Anal. Biochem.* **1976**, *72*, 248−254.

(30) Almeida, T. S.; Garbim, C.; Silva, R. G.; De Andrade, A. R. Addition of iron oxide to Pt-based catalyst to enhance the catalytic activity of ethanol electrooxidation. *J. Electroanal. Chem.* **2017**, *796*, 49−56.

(31) Almeida, T. S.; Palma, L. M.; Leonello, P. H.; Morais, C.; Kokoh, K. B.; De Andrade, A. R. An optimization study of PtSn/C catalysts applied to direct ethanol fuel cell: Effect of the preparation method on the electrocatalytic activity of the catalysts. *J. Power Sources* **2012**, *215*, 53−62.

(32) Palma, L. M.; Almeida, T. S.; de Andrade, A. R. Comparative study of catalyst effect on ethanol electrooxidation in alkaline medium: Pt- and Pd-based catalysts containing Sn and Ru. *J. Electroanal. Chem.* **2020**, *878*, 114592.

(33) Moehlenbrock, M. J.; Minteer, S. D. Extended lifetime biofuel cells. *Chem. Soc. Rev.* **2008**, *37*, 1188−1196.

(34) Antolini, E.; Colmati, F.; Gonzalez, E. R. Ethanol oxidation on carbon supported (PtSn)alloy/SnO2 and (PtSnPd)alloy/SnO2 catalysts with a fixed Pt/SnO2 atomic ratio: Effect of the alloy phase characteristics. *J. Power Sources* **2009**, *193*, 555−561.

(35) Liu, Y.; Hu, P.; Wei, M.; Wang, C. Electrocatalytic Study of Ethylene Glycol Oxidation on Pt 3 Sn Alloy Nanoparticles. *ChemElectroChem* **2019**, *6*, 1004−1008.

(36) Sieben, J. M.; Duarte, M. M. E. Nanostructured Pt and Pt−Sn catalysts supported on oxidized carbon nanotubes for ethanol and ethylene glycol electro-oxidation. *Int. J. Hydrogen Energy* **2011**, *36*, 3313−3321.

(37) Colmati, F.; Antolini, E.; Gonzalez, E. R. Effect of temperature on the mechanism of ethanol oxidation on carbon supported Pt, PtRu and Pt3Sn electrocatalysts. *J. Power Sources* **2006**, *157*, 98−103.

(38) Luo, S.; Chen, W.; Cheng, Y.; Song, X.; Wu, Q.; Li, L.; Wu, X.; Wu, T.; Li, M.; Yang, Q.; Deng, K.; Quan, Z. Trimetallic Synergy in Intermetallic PtSnBi Nanoplates Boosts Formic Acid Oxidation. *Adv. Mater.* **2019**, *31*, 1903683.

(39) Stevanović, S.; Tripković, D.; Tripković, V.; Minić, D.; Gavrilović, A.; Tripković, A.; Jovanović, V. M. Insight into the Effect of Sn on CO and Formic Acid Oxidation at PtSn Catalysts. *J. Phys. Chem. C* **2014**, *118*, 278−289.

(40) Serov, A.; Kwak, C. Recent achievements in direct ethylene glycol fuel cells (DEGFC). *Appl. Catal., B* **2010**, *97*, 1−12.

(41) Da Silva, R. G.; Rodrigues de Andrade, A.; Servat, K.; Morais, C.; Napporn, T. W.; Kokoh, K. B. Insight into the Electrooxidation Mechanism of Ethylene Glycol on Palladium-Based Nanocatalysts: In Situ FTIRS and LC-MS Analysis. *ChemElectroChem* **2020**, *7*, 4326−4335.

(42) Falase, A.; Garcia, K.; Lau, C.; Atanassov, P. Electrochemical and in situ IR characterization of PtRu catalysts for complete oxidation of ethylene glycol and glycerol. *Electrochem. Commun.* **2011**, *13*, 1488−1491.

(43) Franco, J. H.; Grattieri, M.; de Andrade, A. R.; Minteer, S. D. Unveiling complete lactate oxidation through a hybrid catalytic cascade. *Electrochim. Acta* **2021**, *376*, 138044.

(44) Franco, J. H.; Klunder, K. J.; Russell, V.; de Andrade, A. R.; Minteer, S. D. Hybrid enzymatic and organic catalyst cascade for enhanced complete oxidation of ethanol in an electrochemical micro-reactor device. *Electrochim. Acta* **2020**, *331*, 135254.

(45) Zhang, L.; Bai, L.; Xu, M.; Han, L.; Dong, S. High performance ethanol/air biofuel cells with both the visible-light driven anode and cathode. *Nano Energy* **2015**, *11*, 48−55.

(46) Aquino Neto, S.; Almeida, T. S.; Belnap, D. M.; Minteer, S. D.; De Andrade, A. R. Enhanced Reduced Nicotinamide Adenine Dinucleotide electrocatalysis onto multi-walled carbon nanotubes-decorated gold nanoparticles and their use in hybrid biofuel cell. *J. Power Sources* **2015**, *273*, 1065−1072.

(47) Bonfin, C. S.; Franco, J. H.; de Andrade, A. R. Ethanol bioelectrooxidation in a robust poly(methylene green-pyrrole)-mediated enzymatic biofuel cell. *J. Electroanal. Chem.* **2019**, *844*, 43−48.

(48) Topcagic, S.; Minteer, S. D. Development of a membraneless ethanol/oxygen biofuel cell. *Electrochim. Acta* **2006**, *51*, 2168−2172.